



Page 1 hour per response, including the time for reviewing instructions, searching existing data sources, gathering the necessary data, reviewing the collection of information, Send comments regarding this burden estimate or any other aspect of this collection of information, including suggestions for reducing this burden, to Washington Headquarters Service, Directorate for Information Operations and Reports, 1215 Jefferson Avenue, Washington, DC 20540

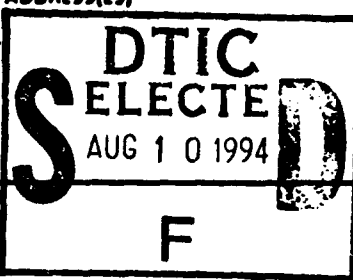
1. DATE: June 15, 1994 3. REPORT TYPE AND DATES COVERED

4. TITLE AND SUBTITLE: Poling Dynamics and Relaxation of Polar Order in Guest/Host Polymers by Second Harmonic Generation 5. FUNDING NUMBERS: #313H030 Kenneth J. Wynne

6. AUTHOR(S): H.W. Guan, C.H. Wang and S.H. Gu

7. PERFORMING ORGANIZATION NAME(S) AND ADDRESS(ES): University of Nebraska-Lincoln, 632 Hamilton Hall, University of Nebraska, Lincoln, NE 68588-0304 8. PERFORMING ORGANIZATION REPORT NUMBER: #26

9. SPONSORING/MONITORING AGENCY NAME(S) AND ADDRESS(ES): Office of Naval Research, 800 N. Quincy Street, Arlington, VA 22217-5000 10. SPONSORING/MONITORING AGENCY REPORT NUMBER: Office of Naval Research



11. SUPPLEMENTARY NOTES: The Journal of Chemical Physics

12a. DISTRIBUTION/AVAILABILITY STATEMENT: This document has been approved for public release and sale; its distribution is unlimited. DTIC QUALITY INSPECTED

A detailed study of the decay of the second-harmonic generation (SHG) signals of several guest-host nonlinear optical polymer systems has been carried out. The decay of the SHG signal is found to be affected by surface and trapped space charges. A fast component is observed at a low poling field and is found to be mainly due to surface charges which orient the chromophores near the surface. A second component, associated with macroscopic polarization, is induced at high field. The intensity of the second component, which decays considerably slower than the fast component, rapidly increases when the poling field is greater than a threshold voltage. Above the temperature of glass transition, T_g, a single exponential function gives a good fit to the shape of the second component of the SHG intensity decay curve. The time constant of the slow component is found to increase with successive poling-decay cycles and reaches a steady state value after several cycles have been performed. This lengthening effect is found both above and below T_g. Furthermore, the relaxation time of the slow component is found also to depend on the poling field strength. The temperature dependence of the steady state relaxation time is not Arrhenius; the Vogel-Fulcher-Tammann equation gives a satisfactory fit to the temperature dependence data.

14 SUBJECT TERMS: Nonlinear Optical NLO polymer, Second Harmonic Generation, Poling Dynamics of NLO Polymer, Dipolar Order and Relaxation, Field Dependence, Temperature Dependence. 15. NUMBER OF PAGES 16. PRICE CODE

17 SECURITY CLASSIFICATION OF REPORT: Unclassified 18 SECURITY CLASSIFICATION OF THIS PAGE: Unclassified 19 SECURITY CLASSIFICATION OF ABSTRACT: Unclassified 20. LIMITATION OF ABSTRACT

94-19232

94 8 60 689

248

**POLING DYNAMICS AND RELAXATION OF POLAR
ORDER IN GUEST/HOST POLYMERS BY SECOND HARMONIC GENERATION**

H. W. Guan, C. H. Wang* and S. H. Gu

*Department of Chemistry
University of Nebraska-Lincoln
Lincoln, NE 68588-0304 USA*

Accession For	
NTIS CRA&I DTIC TAB Unannounced Justification	
By <i>Perlti</i> Distribution/	
Availability Codes	
Dist	Avail and/or Special
<i>A-1</i>	

* To whom all communication should be addressed.

Abstract

A detailed study of the decay of the second-harmonic generation (SHG) signals of several guest-host nonlinear optical polymer systems has been carried out. The decay of the SHG signal is found to be affected by surface and trapped space charges. A fast component is observed at a low poling field and is found to be mainly due to surface charges which orient the chromophores near the surface. A second component, associated with macroscopic polarization, is induced at high field. The intensity of the second component, which decays considerably slower than the fast component, rapidly increases when the poling field is greater than a threshold voltage. Above the temperature of glass transition, T_g , a single exponential function gives a good fit to the shape of the second component of the SHG intensity decay curve. The time constant of the slow component is found to increase with successive poling-decay cycles and reaches a steady state value after several cycles have been performed. This lengthening effect is found both above and below T_g . Furthermore, the relaxation time of the slow component is found also to depend on the poling field strength: when the host is polymethylmethacrylate, it is found that the relaxation time increases with increasing poling field strength; on the other hand, it decreases with the poling field when polysulfone is used as the host. The temperature dependence of the steady state relaxation time is not Arrhenius; the Vogel-Fulcher-Tammann equation gives a satisfactory fit to the temperature dependence data.

Introduction

Because of their potential applications in integrated optics, interest in polymeric nonlinear optical (NLO) materials has grown rapidly during the past decade.¹ It has been well established that molecules containing an electron donor-acceptor, attached to a π -conjugated system exhibit large quadratic hyperpolarizabilities. Due to ease in processability as well as considerable durability and flexibility, polymeric materials, either doped or covalently bonded with NLO chromophores, have been considered as promising candidates for applications.² By incorporating these molecules into the polymer system and then polarizing them with a strong DC electric field to remove centrosymmetry, one can prepare a second-order NLO material. The electric field polarizing process is known as poling.

In the poling process, the polymeric material containing the NLO chromophores is heated to a temperature in the vicinity of the glass transition temperature T_g ; a strong DC electric field is then applied to align the NLO chromophores to achieve a maximum polar order. The polymer is then cooled in the presence of the poling field which is removed when the system reaches room temperature. The result of optimum polar orientational order thus depends on three major parameters: temperature, poling time and strength of the electric field.

Study of the temporal stability of the NLO polymer as the temperature is changed has been reported;^{3,4} however, very few investigations into poling dynamics have been carried out. The ions or electrons injected into the bulk polymer associated with corona or contact electrode poling complicate the understanding of the poling process and subsequent orientational decay. Kohler et al have reported on the second harmonic generation (SHG) and thermally stimulated currents (TSC) in NLO polymers.⁵ They have found in the TSC

measurements that, in addition to the reorientation of the NLO dipoles, drifting space charge and charges that were injected by the electrodes are also present. By simultaneously measuring SHG and TSC signals with increasing temperature, they have found that the SHG signal disappears before the onset of the relaxation of the injected charges. Stähelin et al³ also investigated the mechanism of dipolar reorientation in several guest/host systems. They monitored the change in the SHG signal in connection with different poling sources, poling geometries and electrode materials; they observed little difference in the decay of the SHG signal from different methods of poling.

For application in frequency doubling or electro-optic devices, the polymer must be poled in order to yield optimum polar order and the polar order created near the glass transition temperature of the NLO polymer must be maintained. Therefore, an understanding of the dynamics of poling as well as underlying mechanisms responsible for the relaxation of polar orientational order is of great interest. In this paper we report new results from our laboratory concerning poling dynamics, the effects of temperature change, and the dependence of the relaxation behavior on the electric field for guest/host polymers. The study of the guest/host polymers is of great interest because it provides clear information regarding the physics of NLO chromophores in a polymeric environment. In addition, it also yields information that contributes to a better understanding of the parameters needed in applications with good temporal stability with high T_g polymers (such as polyimides) serving as hosts.

EXPERIMENTAL

Nitroaminostilbene (NAS) and nitroaminotolane (NAT) were synthesized in our laboratory. NAS and NAT were used as NLO chromophores, and the host polymers used in this work were polymethylmethacrylate (PMMA) ($M_w > 100$ K, Aldrich) and polysulfone

(PSF) ($M_w \approx 67,000$, Aldrich).

The host polymers were dissolved in appropriate solvents. Various amounts of NLO chromophores were dissolved in the polymer solution to obtain different NLO concentrations. The solutions were filtered to remove undissolved particulates. Thin, optically clear films (about 1-2 μm thickness; film thickness was measured with an α -stepper) were prepared by spin coating the solution onto transparent conducting substrates (indium tin oxide, ITO, coated soda lime glass slides). The ITO coated slides with polymer films were first placed in a vacuum oven at about 50°C for over 24 hrs and then baked for another 24 hrs at a higher temperature (slightly above T_g) to obtain solvent-free films. The glass transition temperatures, T_g , of all films were determined by a differential scanning calorimeter (DSC, Perkin Elmer delta series). In the NAS/PMMA system no evidence of phase separation was initially observed for samples containing up to 30 weight % of NAS. However, after several cyclings of the poling-cooling steps, phase separation occurred for films containing more than 15 weight % of NAS in PMMA; many small NAS crystallites dispersed in the PMMA matrix were then found. The solubility of NAT in PMMA is considerably lower. The concentration of the chromophores in homogeneous films was monitored by UV-visible absorption spectroscopy. Two types of poling techniques (contact and corona discharge) were studied. For experiments dealing with contact electrode poling, two glass slides spin-coated with NLO polymer film were fused in a sandwich configuration by placing them together in a vacuum oven at a temperature exceeding T_g . For corona poling, a positive voltage of less than 3 kV was applied to a sharp tungsten needle located 1 cm in front of the polymer film surface. Both the contact poling and corona poling procedures were conducted in dry air in an oven which housed the sample. Establishment of polar order as a result of poling and subsequent relaxation of the polar order were monitored by measuring the SHG signal. The optical

measurements were carried out at the same temperature as the poling process. The setup for SHG measurement was similar to that used in our previous work.⁶ Basically, it consisted of a Q-switched Nd:YAG laser operated at 10 Hz. The fundamental beam at 1.064 μm was incident on the sample with the polarization in the plane of incidence and the SHG intensity of each sample was referenced to quartz. The intensity was detected with a PM tube and processed with a boxcar integrator which was interfaced to a personal computer.

Results and Discussion

The SHG signal is proportional to the square of the second order optical susceptibility $\chi^{(2)}$, which in the case of an electric-field poled amorphous NLO polymer consists of only two components $\chi_{33}^{(2)}$ and $\chi_{31}^{(2)}$. For a molecule with a dominant β element, one can show that if the field-dipole interaction is less than kT , $\chi_{31}^{(2)}$ is equal to $\chi_{33}^{(2)}/3$, regardless of the type of intermolecular interaction present⁷. On the other hand, $\chi_{33}^{(2)}$ is larger than $\chi_{31}^{(2)}/3$ if the poling field is large such that the field-dipole interaction is greater than kT .² The study of the decay of the SHG signal provides information on the time dependence of $\chi^{(2)}$ as a result of the reorientation of the chromophore dipoles.

We show in the top of Fig. 1 the rise portion of the SHG signal for a sample with 2.4 weight % NAS dissolved in PMMA. The sample was poled with the corona discharge method, with trace (I) poled at 2.8 kV and trace (II) poled at 4.0 kV. The sample was poled at 100°C, and the decay was measured at the same temperature. One notes that the signal rise is much faster when a higher voltage is used. Nearly an instantaneous rise and then a rapid establishment of a steady state signal is found in the 4.0 kV case, whereas the signal rise associated with the 2.8 kV poling voltage is gradual and it takes several hundred seconds to reach the steady state. In addition, the SHG signal is considerably larger for the sample

poled at 4 kV than at 2.8 kV. One also notes that when the corona voltage is small, the signal rise is not smooth; several "bumps" in curve (I) are clearly seen. These bumps are presumably associated with the redistribution of the surface charges that are deposited on the polymer film surface. However, the surface charge redistribution is considerably faster when a higher poling voltage is used, as shown in the rapid smooth signal rise in trace (II).

After the SHG signal reaches a steady state value, the poling voltage is turned off. The signal then decays, as shown in the bottom portion of Fig 1. One notes that the decay characteristics of the SHG signal also depends on the poling voltage. The decay is slower when the sample is poled at 2.8 kV than when it is poled at 4.0 kV, as clearly shown by traces (I) and (II) in the bottom of Fig 1, respectively. In both cases the decay behavior is not single exponential. Best fits of $\chi^{(2)}$ (proportional to square root of the SHG intensity) data to the Kohlrausch-Williams-Watts (KWW) function (the stretched exponential) given by

$$\chi^{(2)} = a e^{-(t/\tau)^\gamma} \quad (1)$$

yield values for τ and γ . Here τ is the characteristic relaxation time, and γ is the width parameter whose value is $0 \leq \gamma \leq 1$. Values of γ and τ for the film poled with 2.8 kV are 0.65 and 419.2 sec, respectively. On the other hand, values of γ and τ for the 4.0 kV case are 0.89 and 700.1 sec respectively. Thus, the film poled with a lower voltage has a wider distribution of relaxation times as well as a shorter characteristic relaxation time τ . The average relaxation time $\langle \tau \rangle$ associated with trace (I) is 574.0 sec, in comparison with $\langle \tau \rangle = 739.5$ sec for trace (II). The average relaxation times are calculated using the expression

$$\langle \tau \rangle = \tau \Gamma(1/\gamma)/\gamma \quad (2)$$

The time dependence of $\chi^{(2)}$ after the poling field is removed, as represented by the

decay of the SHG signal, is due to reorientation of the electric dipoles, resulting in the decrease of polar orientational order. The KWW functional representation suggests that the decay has either a distribution of relaxation times or has a complex nonexponential single relaxation process. The former case corresponds to inhomogeneous distribution of relaxation times and the latter case can be considered as due to a homogeneous nonexponential relaxation mechanism. We believe it is the combination of both in the case of SHG signal decay, owing to the fact that both nonuniform distribution of surface charges and trapped charges play a role in affecting the relaxation of polar order.

It is known that when a voltage is applied to a two-layer dielectric consisting of a layer with mobile ions and an insulating layer, a region with space-charge will be built up at the interface between the two layers due to the migration of mobile ions⁸. The space charge will create a static electric field, which might prolongs the decay of $\chi^{(2)}$ ⁹. For *in situ* corona poling, positive ions continue to be deposited on the polymer film, some of which are transported across the film. When the poling is stopped and the polymer cooled down, these ions might be trapped as space charges, and the decay of space charges could affect the relaxation of the SHG signal. As shown by Köhler⁵, trapped charges are released at temperatures higher than the onset of dipolar orientational relaxation, and in the time regime that the space charge relaxation occurs, the SHG signal already decays completely. Thus, the effect of space charges is always present during the course of the SHG decay. However, without a detailed knowledge of concentration of mobile ions, impurities, and the dynamics of the space charge decay, it is difficult to quantitatively separate out the space charge contribution to the SHG intensity decay behavior. The contact electrode poling method provides another method of studying the relaxation behavior of $\chi^{(2)}$ after the poling field is turned off. In the contact electrode poling method, the surface charges built up at the

interface can be readily bled off by short-circuiting the electrodes. However, the injected space charges that might be trapped in the bulk when the poling voltage is removed are still present in the contact electrode poling technique. The advantage of the contact electrode poling technique is that the field strength to which the polymer film is subjected can be readily determined.

In Fig. 2 we show the SHG intensity relaxation curves obtained for the 5 weight % NAS in PMMA sample poled at 110°C using the contact electrode poling technique under two different field strengths. At the field strength of about 7.2×10^5 V/cm, two components are clearly evident (Fig. 2a or 2b), but at a higher field strength, 9.0×10^5 V/cm, only one component is clearly observed (2c or 2d); the short time component is nearly covered by the stronger long time component. The relaxation curve shown in (Fig. 2a or 2b) can also be fit satisfactorily with the sum of two single exponentials, with one single exponential representing each relaxation component. Similarly, a single exponential is sufficient to fit the curve (Fig. 2c or 2d) provided that the short time component is excluded. One notes that the two-exponential decay curve shown in Fig. 2b is clearly displayed when the time axis is set in the logarithmic scale. Thus, except for the short time portion, a single exponential decay curve fits rather satisfactorily the decay curve portrayed in Fig 2d. On the other hand, one can also force fit the whole decay curve in terms of a KWW function with a γ parameter equal to about 0.26, consistent with that reported previously.^{4,10} However, a two single exponential fit gives a smaller standard deviation. The two exponential fit was also considered in ref. 9.

We consider causes for the two single exponential decay observed in Fig. 2a-2d. While the fast decay may involve several mechanisms, the dominant one is due to the effect of surface charges. In Fig. 3, we show a detailed "shot to shot" plot of the SHG signal for

the 10 weight % NAS/PMMA sample poled at 96°C after the poling field is turned off. The data shown in Figs. 3 and 4 are poled at the voltage less than the threshold voltage (see below for the definition for the threshold voltage). In trace (a) electrodes are shorted immediately after the poling field is turned off. In this case, the SHG signal takes a step-wise decrease to the background. Traces (b) and (c) correspond to the decays with a $10^5 \Omega$ and a $10^{10} \Omega$ resistor connected to the cathode, respectively. Clearly, the signals represented by these curves decay gradually, with the $10^{10} \Omega$ resistor case decaying with a longer time constant.

The effect of surface changes is more clearly displayed if poling is carried out at even lower voltage. In Figs. 4a and 4b the shot to shot SHG signal is again shown for the 5 weight % NAT/PMMA sample poled at 109°C subjected to 250 V (corresponding to a field of 7.8×10^5 V/cm). At this poling voltage the SHG signal rapidly drops to zero when the electrodes are shorted immediately after the poling field is turned off (Fig. 4a); on the other hand, if the electrodes are not shorted, the SHG signal assumes a gradual decay (Fig. 4b). The time of decay closely follows the field switching-off time. In both Figs. 3 and 4, only the fast decay portion is observed.

It should be noted that by increasing the poling field, a second, slower component appears. Shown in Fig. 5 is the SHG signal of the same sample poled with a higher voltage (450 V or 1.4×10^6 V/cm). At this poling voltage, the SHG signal does not drop to zero but to about 1/3 of the initial signal after the poling field is turned off and the electrodes shorted. One notes that after the precipitous initial drop a slow decaying signal follows.

The separation of the fast and slow components is much clearer if the experiment is carried out at temperatures lower than T_g . By cooling the sample to 89°C, we were able to separate the two components and obtain the intensity of fast and slow components as a

function of poling voltage. The SHG intensities of the fast and slow components for 5 weight % NAT/PMMA and for 5 weight % NAS/PMMA samples are plotted as a function of poling field, E_p , in Fig 6. It appears that there exists a threshold voltage or threshold field, E_{th} , above which the slow component becomes visible. Below the E_{th} , the SHG intensity is due only to the fast component. Above the E_{th} , the intensity of the fast component decreases with increasing field strength whereas the intensity of the slow component increases with increasing poling field. For the NAT/PMMA sample, the slow component is several hundred times more intense than the fast component when E_p is equal to 1.65×10^6 V/cm, and becomes even stronger at high field strength (c.f. the top of Fig 6). For the NAS/PMMA sample, the slow component dominates the SHG intensity for field greater than 9×10^5 V/cm (c.f. the bottom of Fig 6, the fast component is not shown due to its small relative intensity).

We have monitored the current passing through the sample during the poling process. Shown in the inset of Fig. 6 are the currents due to drifting space charges as a function of poling voltage for the NAT and NAS samples discussed above. Below the threshold field, E_{sh} , the current flowing through the sample is less than 40 nA, but above E_{sh} it increases steadily with increasing voltage until discharge occurs, resulting in break-down of the sample. The fact that current is present even for the voltage below the threshold voltage (V_{th}) indicates that the work function of ITO is less than eV_{th} , where e is the charge. To decrease the correlation of trapped charges, selection of the electrodes with high work function is thus preferred. However, the presences of trapped charges appears to prolong the SHG decay and stabilize the signal (see below).

While the current is expected to depolarize the induced polarization, it is interesting to note that the amplitude of the SHG signal associated with the slow component is proportional to the depolarization current. The resistance of the sample is about $1-2 \times 10^9$ ohms, and the

depolarization due to the current is thus completely compensated by the increase in the poling field and results in large polar order in the medium. However, it should be emphasized that in contact electrode poling, the SHG intensity is measured after the poling field is turned off. After the poling field is turned off there is only negligible current flowing through the sample (not measurable with a nanoammeter). As the poling field is removed, the drifting space charges become trapped in the sample, and unless these trapped charges find a pathway to decay away before the decay of the macroscopic nonlinear polarization, the decay of SHG signal will be affected by the trapped charges. However, according to reference 5, the trapped charges decay after the induced NLO chromophore orientation relaxes. Thus the SHG decay is always affected by the trapped surface charges.

These results thus show that the fast component of the decay curve is closely associated with the surface charges produced at the cathode and the slow component is due to reorientation of NLO chromophore which is affected by trapped space charges. These surface charges polarize the dipoles of the chromophores near the surface of the film. As a result of the rapid decay of surface charge, it is not difficult to see that at high voltages and at high temperatures ($T > T_g$) the SHG signal from the surface dipoles will relax with a shorter time constant than that associated with the macroscopic polarization induced in the bulk. Consequently, the fast decay component which is only barely apparent in Figure 2d is nearly covered by the dominant slower decay component.

Due to the fact that the fast decay is closely associated with the surface charges, the study of the orientation of the dipoles induced near the surface would require constructing faster switching electronic circuitry to rapidly turn on and off the poling field. We concentrate in the present work on the study of the second slower decay component associated with the relaxation of the macroscopic polarization. In the contact poling method,

the relaxation of the induced macroscopic polarization will not be affected by the surface charges as they are bled off by shorting the electrodes.

Clearly the relaxation of the major component of the SHG signal is associated with the fluctuations of macroscopic polarization due to the collective dipolar reorientation of the NLO chromophores in the bulk. In general, the orientation dynamics of the chromophores are rather complex and individual chromophore orientation is expected to occur over a range of time scales. However, as pointed out above, since the trapped charges take a longer time to decay, these chromophores will be correlated by the trapped charges and the relaxation of the macroscopic NLO polarization is thus prolonged by the presence of trapped charges.

We have observed an interesting memory effect associated with the establishment of the NLO macroscopic polarization. Shown in Fig. 7 is a series of SHG relaxation curves for the NAS/PMMA sample (5 weight % NAS) at 100°C. Curve (a) resulted from the sample being poled with a field of 8.4×10^5 V/cm. After the SHG signal decays completely, the poling field with the same strength is turned on and, within a few seconds, an SHG intensity of about the same initial level is recovered. However, after the poling field is turned off, the SHG decay is found to become longer than the previous one, as shown in (b). As the process is repeated, the relaxation times become successively longer until a plateau value of the relaxation time about 4000s is obtained for the sample poled at this field strength. After the plateau value is reached, there is no longer any change in the decay curve, regardless of the number of times that the sample is repoled. These results are also observed for the sample above T_g , but the relaxation time lengthening effect above T_g is considerably reduced in the NAS/PMMA sample. The relaxation time lengthening effect observed below T_g is expected to be also affected by the physical aging mechanism of the NLO polymer.

The NAS/polysulfone (PSF) sample also displays a pronounced relaxation time

lengthening effect above T_g . In Fig. 8 we show a 5 weight % NAS/PSF sample poled with 490 Volts at 184°C, which is more than 30°C above T_g (150.6 °C). In this case, the effect of physical aging will not play a role in the lengthening of the relaxation time. One notes that the SHG decay time constant gradually increases as the sample is successfully poled (going from the top to bottom in Figure 8).

While we do not at present have a quantitative theory for the effect, we offer a qualitative explanation of the observation. By poling, the dipoles overcome the viscous barrier of the surrounding polymer to orient along the electric field direction. However, due to the high poling field, charges (electrons in contact poling and positive ions in corona poling) are present in the medium, thereby modifying its dielectric properties. Since the medium is also elastic (considering the fact that the polymer system is viscoelastic), the elastic stress induced by the poling field and trapped charges owing to electrostriction also helps align the dipoles. Since the elastic response is much faster than the viscous response, this explains why the medium can be repoled rapidly after the SHG signal has decayed. The lengthening of the relaxation is presumably associated with the injected charges trapped in the sample. As mentioned above, due to the charge-dipole interaction, the presence of the trapped charges is expected to correlate the chromophore dipoles, thereby reducing the range of time scales as the dipolar relaxation now taking place cooperatively. The enhancement of polar orientational correlation via trapped charges is expected to lead to the lengthening of the SHG relaxation time. Since the trapped charges have a life-time longer than the relaxation time of the SHG,⁵ the effect of the trapped charges is present throughout the duration of the SHG decay. Additional charges are injected into the medium following each poling cycle. As a result, the SHG signal relaxation will become longer as the system is repoled. However, once the medium is saturated with charges after several poling cycles, no

more trapped charges can be injected into the medium and hence a plateau SHG relaxation time will be obtained. Thus, as the system is repoled, more and more chromophores are correlated by the trapped charges and the SHG signal will assume a progressively longer decay until the plateau relaxation time is obtained.

If the temperature of the NLO polymer is below T_g , one expects that physical aging also plays a role because the effect of isothermal annealing between successive poling stages is expected to densify the polymer, hence increasing the relaxation time. A signature of the effect of physical aging on the relaxation time is the power law dependence of the relaxation time τ versus aging time t_a .¹¹ We present in Fig. 9 the log-log plot of τ vs. t_a to show the $\tau = At_a^{-\gamma}$ dependence that was observed; although the data are rather scattered, clearly the power law dependence is approximately obeyed. However, the value obtained for the exponent ($\gamma = 0.68$) is less than 1 and indicates that it is associated with the early stage of physical aging.¹¹ In Fig. 9, the aging time, t_a , is taken as the elapsed time after the initial poling.

We have studied the steady state plateau relaxation time as a function of temperature. The temperature dependence does not obey Arrhenius type of behavior, but instead displays a Vogel-Fulcher-Tammann (VFT) (or equivalently the Williams-Landel-Ferry (WLF)) form

$$\tau(T) = \tau_{\infty} \exp [B/(T - T_0)], \quad T > T_0 \quad (3)$$

as shown in Fig. 10 for 1 and 5 wt. % NAS/PMMA samples. Fitting the relaxation time data to Eq. (2) for the 5 weight % NAS/PMMA sample, gives $\tau_{\infty} = 6.8 \times 10^{-8}$ s and $T_0 = 293$ K, but for the 1 weight % NAS/PMMA sample, we obtain $\tau_{\infty} = 3.4 \times 10^{-5}$ s and $T_0 = 301$ K. Two remarks are in order. Since the WLF parameter C_2 is equal to $T_g - T_0$ we can convert T_0 to C_2 and find out how the C_2 value varies as the chromophore concentration is changed. From the T_g data, we obtain for the 5 weight % sample a C_2 value equal to 90 K, and for

the 1 weight % sample $C_2 = 80$ K, which equals the C_2 value for pure PMMA reported in the literature¹². The C_2 value will increase as the polymer is plasticized. Furthermore, the τ_∞ value is much longer for the 1% than 5% NAS sample, again consistent with the effect of plasticization. The other remark is the VFT equation appears to describe all data above and below T_g . This is in contrast to the result of reference 4, which shows that different equations are needed to describe results above and below T_g .

It should be noted that the rise in the SHG signal during the poling stage and the signal decay after the poling field is turned off have a different time response, in contrast to the result previously reported.¹³ Certainly, in the case of linear response and also in the absence of trapped charges that modify the internal field, one would expect the same reorientational dynamics to be responsible for both the rise and the decay, and thus one expects the rise time and relaxation time to be similar. However, under a strong poling field and in the presence of trapped charges, we do not anticipate the rise and decay portions of the SHG signal to have the same time scale. In fact, all results of our studies have shown that the SHG intensity reaches its maximum plateau value within a few seconds; whereas, after the field is turned off, the SHG intensity takes a much longer time to decay (see Fig. 1). The slower decay is the result of strong dipolar orientational correlation induced by poling, as well as the trapped charges which modify the internal field and prevent the reorientation of the dipoles. In previous work, we showed that the dipolar orientational correlation effect could assist the dipolar orientation⁶, and also give rise to a relaxation time lengthening¹⁴ effect when the poling field strength is increased.

It is possible to understand the field dependence by considering that the average orientational relaxation rate τ^{-1} is related to the mobility, μ , and the second order susceptibility, $\chi^{(2)}$ by¹⁴

$$\chi^{-1} = \mu / \chi^{(2)} \quad (4)$$

Since $\chi^{(2)}$ increases with the poling field strength and is proportional to the orientational pair correlation factor, one expects that the orientational relaxation time τ would increase with the poling field E_p , provided that the mobility μ is not affected by the electric poling field. Our results for NAS/PMMA and NAT/PMMA show that this is indeed the situation for a poling field of about 10^6 V/cm. The results for the field dependence of the relaxation of NAS/PMMA are already reported in reference 14. Shown in Figure 11 is the voltage dependence of the NAT/PMMA sample, which clearly shows that τ also increases with the poling voltage. On the other hand, if the internal field due to the combined effect of poling and trapped charges also affects the mobility μ , then τ may increase or decrease with increasing E_p , depending on the relative effect of the internal field on μ and $\chi^{(2)}$. If the increase in E_p causes the polymer chain to be more mobile due to the change in the internal field and if the field effect on μ is greater than the increase of $\chi^{(2)}$, then a decrease in the relaxation time τ would result. Shown in Figure 12 is the field dependence of τ for the 5 weight % NAS/PSF sample at 183°C , which is 33°C above T_g (150°C). Clearly the relaxation time decreases with increasing E_p , in contrast to the cases of NAS/PMMA and NAT/PMMA in which τ is found to increase with increasing E_p . Since the polysulfone chain contain phenyl rings, which have a propensity for trapping electrons, it is not surprising that the polymer chain mobility is affected by the trapped electrons, in contrast to the aliphatic constituent of the PMMA chains. Thus, the decrease of τ with E_p observed in the PSF system is presumably due to the effect of trapped electrons by which the mobility of the PSF chains is greatly increased. It is interesting to note that trapped electrons do not significantly affect the NLO chromophore electronic structure, because if they did, the SHG intensity would be reduced. We did not observe the SHG intensity reduction due to electron injection.

Finally, we should mention that the steady state relaxation times τ that we have measured for the charge transfer chromophores in various polymer hosts are longer by at least two orders of magnitude than that reported by Dhinojwala, et al¹³ where a repetitive pulsed poling field with the pulsed field spacing variable from 200 μ s to 0.5 s was used. In their work, they have not discussed the effects due to surface charges nor have they considered the relaxation time lengthening effect that we have observed. Also, no allowance is provided to remove the surface charge in their work. Furthermore, the poling field strength used by Dhinojwala et al. is only about 3.2×10^2 V/cm, which is nearly four orders of magnitude less than the poling field that we have employed in the present work. From the discussion given above, it is certain that results reported in ref. 13 correspond to the fast decay component, associated with the dipolar orientation induced by the surface charges. As has previously been shown,⁵ the slower collective macroscopic polarization component cannot be induced at such a weak field. The effect of the poling field on lengthening the relaxation was also previously noted by Ye et al,¹⁶ but they did not provide experimental data nor discuss its cause.

In summary, we have carried out a detailed investigation of the decay of the SHG signals of several guest host NLO polymer systems. The decay of the SHG signal is found to be affected by surface and trapped space charges. A fast component is observed at a low poling field, and is found to arise mainly from the orientation of dipoles near the surface. Removing the surface charges also removes this fast component. A second component associated with the decay of macroscopic polarization is induced at high field. The decay of the second component is considerably slower than the fast component. As the strength of the poling field is increased, we have found that the amplitude of the fast component decreases and the slower component increases. Above T_g , a single exponential function gives an

excellent fit to the shape of the decay of the second SHG component. A memory effect associated with the second component has also been observed in several samples above and below T_g , with the memory effect being more pronounced for samples at temperature below T_g . The time constant of the second slow component is found to successively increase with the poling-decay cycle, reaching a plateau value after several cycles. The steady state relaxation time has been found to depend on the poling field strength E_p . In the NAS/PMMA and NAT/PMMA systems, the relaxation time of the slow component increases with increasing E_p , but in the NAS/PSF system it decreases with increasing E_p . The memory effect and the poling field dependence have been interpreted as due to the combined effects of pair orientational correlation of dipoles and orientational mobility. The results suggest that the orientational mobility of PMMA chains are not affected by the internal field, but the mobility of the PSF chain is considerably affected. The temperature dependence of the steady state relaxation time is not Arrhenius. The Vogel-Fulcher-Tammann equation gives a satisfactory fit to temperature dependence relaxation time data.

Acknowledgement: This work is supported by the Office of Naval Research. We thank Mr. Mark A. Pauley for proof reading the manuscript and for technical assistance.

References

1. J. Zyss, *J. Mol. Electron.* **1**, 25 (1985).
2. Nonlinear Optical Properties of Organic Molecules and Crystals, D. S. Chemla and J. Zyss, Eds. Academic Press, New York (1987).
3. M. Stähelin, C. A. Walsh, D. M. Burland, R. D. Miller, R. J. Twieg and W. Volksen, *J. Appl. Phys.* **73**, 8471 (1993).
4. C. A. Walsh, D. M. Burland, V. Y. Lee, R. D. Miller, B. A. Smith, R. J. Twieg and W. Volksen, *Macromolecules* **26**, 3720 (1993).
5. W. Köhler, D. R. Robello, P. T. Dao, C. S. Williard and D. J. Williams, *J. Chem. Phys.* **93**, 9157 (1990).
6. H. W. Guan and C. H. Wang, *J. Chem. Phys.* **98**, 3463 (1993).
7. C. H. Wang, *J. Chem. Phys.* **98**, 3457 (1993).
8. E. H. Snow and M. E. Dumesnil, *J. Appl. Phys.* **37**, 2123 (1966).
9. H. L. Hampsch, J. Yang, G. K. Wong, J. M. Tarkelson, *Macromolecules* **23**, 3640 (1990).
10. K. D. Singer, L. A. King, *Poly. Prepr. (Am. Chem. Soc., Div. Polym. Chem.)* **32**, 98 (1991); *J. Appl. Phys.* **70**, 3251 (1991).
11. C. E. Struvik, Physical Aging in Amorphous Polymers and Other Materials, Elsevier Scientific Pub. Co. (1978).
12. G. C. Berry and T. G. Fox, *Adv. Polymer Sci.* **5**, 261 (1967).
13. A. Dhinojwala, G. K. Wong and J. M. Torkelson, *Macromolecules* **25**, 7395 (1992).
14. C. H. Wang, S. H. Gu and H. W. Guan, *J. Chem. Phys.* **99**, 5597 (1993).
15. T. Goodson III and C. H. Wang, *Macromolecules* **26**, 1837 (1993).

16. Ye, C.; Minami, N.; Marks, T.J.; Yang, J., Wong, G. K., *Macromolecules* 1988, 21, 1899.

FIGURE CAPTIONS

- Fig. 1:** Rise (top) and decay (bottom) portions of the SHG signal for the sample with 2.4 wt% NAS dissolved in PMMA poled with a corona discharge method. Trace (I) corresponds to poling at 2.8 KV and Trace (II) at 4.0 KV.
- Fig. 2:** SHG intensity relaxation curves obtained for the 5 wt% NAS in PMMA sample poled under two different field strengths. Intensity relaxation curves displayed in the logarithmic scale (curves b and d) show clearly the fast component.
- Fig. 3:** Shot to shot real time SHG signals for the 10 wt% NAS/PMMA sample poled at 96°C after the poling field is turned off. In (a) electrodes are shorted immediately after the poling field is turned off; (b) and (c) correspond to the decays with $10^5 \Omega$ and $10^{10} \Omega$ resistors connected to the cathode.
- Fig. 4:** Shot to shot SHG signals for the 5 wt% NAT/PMMA sample poled at 109°C subject to a field of 7.8×10^5 V/cm. In (a) electrodes are shorted immediately after the poling field is turned off, in (b) electrodes are not shorted. This figure shows clearly the effect of surface changes.
- Fig. 5:** Same as Fig. 4(a), with the exception that a higher poling field (1.4×10^6 v/cm) is applied. Note that in addition to the fast component, a slow component is also present with a higher poling field.
- Fig. 6:** SHG intensities of the fast (Δ) and slow (\blacktriangle) components for the 5 wt% NAT/PMMA and the 5 wt% NAS/PMMA samples plotted as a function of the poling field E_p . The insets show the current passing through the sample during poling.

- Fig. 7:** SHG decay curves for 5 wt% NAS in PMMA poled below T_g . Note the gradual lengthening of the SHG decay at each successive poling and decay.
- Fig. 8:** SHG decay curves for 5 wt% NAS in PSF poled above T_g to show the gradual lengthening of the SHG decay.
- Fig. 9:** The log-log plot of the SHG relaxation time τ plotted versus aging time t_a for the data shown in Fig. 7
- Fig. 10:** VFT plot of the SHG relaxation time τ to show the non-Arrhenius temperature dependence of τ for 1 and 5 wt% NAS/PMMA samples. Note that C_2 is larger for the 5 wt% sample, thus showing the effect of plasticization owing to the presence of NAS.
- Fig. 11:** Voltage dependence of the SHG relaxation time τ for the 5 wt% NAT/PMMA sample. Note that τ increases with increasing poling voltage.
- Fig. 12:** Voltage dependence of the SHG relaxation time τ for the sample with 5 wt% NAS in PSF at 183°C. ($T_g = 150^\circ\text{C}$). Note that τ decreases with increasing poling voltage for this sample, in contrast to Fig. 11.